Nuclear Instruments and Methods in Physics Research A 810 (2016) 19–26

Contents lists available at ScienceDirect

Nuclear Instruments and Methods in Physics Research A

journal homepage: www.elsevier.com/locate/nima

Influence of magnetic fields on charge sharing caused by diffusion in medipix detectors with a Si sensor

Ako Jamil *, Mykhaylo Filipenko, Thomas Gleixner, Gisela Anton, Thilo Michel

Erlangen Centre for Astroparticle Physics, Friedrich-Alexander-University of Erlangen-Nuremberg, Erwin-Rommel-Strasse 1, 91058 Erlangen, Germany

ARTICLE INFO

Article history:
Received 6 July 2015
Received in revised form
15 November 2015
Accepted 16 November 2015
Available online 28 November 2015

Keywords:
Charge sharing
Solid-state detectors
Magnetic field
Diffusion of charge carriers

ABSTRACT

The spatial and energy resolution of hybrid photon counting pixel detectors like the Timepix detector can suffer from charge sharing. Due to diffusion an initially point-like charge carrier distribution generated by ionizing radiation becomes a typically Gaussian-like distribution when arriving at the pixel electrodes. This leads to loss of charge information in edge pixels if the amount of charge in the pixel fall below the discriminator threshold. In this work we investigated the reduction of charge sharing by applying a magnetic field parallel to the electric drift field inside the sensor layer. The reduction of diffusion by a magnetic field is well known for gases. With realistic assumptions for the mean free path of charge carriers in semiconductors, a similar effect should be observable in solid state materials. We placed a Medipix-2 detector in the magnetic field of a medical MR device with a maximum magnetic field of 3 T and illuminated it with photons and α-particles from ^{241}Am. We observe that with a magnetic field of 3000 mT the mean cluster size is reduced by $\sim 0.75\%$.

1. Introduction

Various experiments seek for the neutrinoless double beta decay ($0\nu\beta\beta$), a hypothetical decay where two neutrons in the nucleus are transformed into two protons and emit 2 electrons. In this decay there are no neutrinos in the final state, which is only possible if $\nu = \overline{\nu}$. According to the Schechter-Valle theorem an observation could prove the Majorana nature of the neutrino independently of the actual process enabling the decay [1,2]. The COBRA collaboration plans to use a large array of Cadmium-Zinc-Telluride (CZT) semiconductor detectors to observe $0\nu\beta\beta$ [3]. Since Cadmium and Tellurium have double beta isotopes, the use of enriched material for the sensitive volume would be the decaying source at the same time. In order to be more sensitive and put a better limit on the half life, of which the current limit is $T_{1/2} \geq 1.9 \cdot 10^{25}$ years [4], large detector masses at the several 100 kg scale are needed. An observation time on the order of some years is necessary. In addition a good energy resolution and very low background is essential.

Instead of using monolithic CZT detectors one can use a Cadmium-Telluride pixel detector, such as the HEXITEC [5] or the Timepix detector [6]. Pixelated detectors have the advantage that background events can be identified by their topological pattern and be rejected afterwards in the data analysis [7–9]. Higher efficiency of particle tracking can be achieved by smaller pixel sizes at the expense of energy resolution which suffers from charge sharing [10]. The effect of charge sharing is due to diffusion of the charge carries during their drift through the sensor. In gases, for instance, the diffusion is known to be reduced by an external magnetic field [11]. We investigated whether this effect can be observed in hybrid photon counting pixel detectors such as the Medipix detector.

2. The medipix detector and theoretical considerations

In this work we were using a Medipix detector, which is a hybrid active pixel detector developed in the Medipix collaboration [12]. The detector consists of the ASIC with 256×256 quadratic pixels and a sensor layer bump bonded on the ASIC by small spherical bonds made of tin. Each pixel has a pixel pitch of 55 µm and has its own analogue and digital units for signal processing [6].

The interaction of an ionizing particle entering the sensor layer leads to the production of e^-h^+ – pairs due to energy loss. The average energy to produce one e^-h^+ – pair is about 3.62 eV in Si [13] and about 4.43 eV in CdTe [14]. An applied bias field drifts the electrons and holes towards the pixel electrodes. While the charge carriers drift they induce mirror charges on the pixel electrode. The amount of charge that is induced is proportional to the traveled difference in the weighting potential [9]. The polarity of the bias is chosen such that the electrons are drifting to the pixel side

* Corresponding author.
E-mail address: ako.jamil@fau.de (A. Jamil).

http://dx.doi.org/10.1016/j.nima.2015.11.117
0168-9002/

and the holes to the common electrode (CdTe sensor) or vice versa (Si sensor).

The induced charge in the pixel electronics is amplified and shaped to a voltage pulse. If the pulse height exceeds a globally set analogue threshold within a given measuring time, called frame, the counter which is present in each pixel is incremented. Energy measurements can be done with a Timepix detector [6], which is a further developed detector for particle physics based on the Medipix detector (Fig. 1).

Initially, the generated charge carrier distribution is almost point-like. Assuming that the pixel array lies in the *x*-*y*-plane, during the drift in *z*-direction a broadening of the charge cloud in *x*-*y*-direction happens. Mainly, two effects contribute to this process. One effect is repulsion, which is due to the repulsive Coulomb force between charges of the same type. The higher the density of the free charge carriers the stronger the contribution from repulsion is. For instance, α-particles with about 5 MeV of energy are highly ionizing and produce a very local high density of charge carriers, which makes repulsion the dominant contribution to charge sharing for their tracks. This leads to a blob like pattern of triggered pixels, as can be seen in Fig. 2. Because of the $1/r$-dependency of the Coulomb potential, the high influence from repulsion at the beginning decreases rapidly during the drift. In contrast to this, the dominating contribution to the broadening of the charge carrier distribution of an electron event comes from diffusion, which is the second major part of charge sharing. Diffusion always occurs when there is some kind of gradient, in this case a carrier concentration gradient. This yields a flux of carriers which, in the case of electrons, can be described by Fick's law. The proportionality constant in the equation is called the diffusion constant, which will be denoted as *D*. Random thermal motion as well as scattering are the cause for this process. The diffusion radius can be estimated as [15]

$$R = \sqrt{2Dt} \approx \sqrt{\frac{z \cdot d}{U}} \quad (1)$$

which depends on the diffusion constant *D*of the sensor material

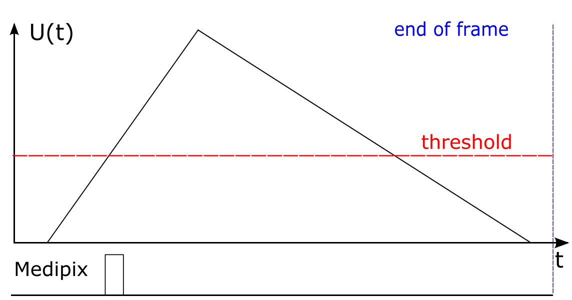

Fig. 1. Schematic view of the Medipix operation mode. A clock pulse is measured if the voltage pulse exceeds the analogue threshold.

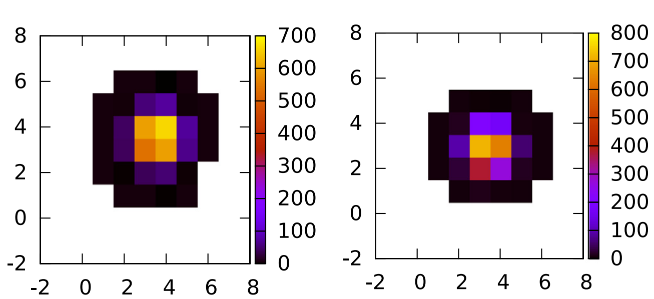

Fig. 2. Typical α-particle event measured with a Timepix detector. The color encodes the energy in keV. Plots are taken from [8]. The x- and y-axis indicate columns and rows of the pixel matrix.(For interpretation of the references to color in this figure legend, the reader is referred to the web version of this article.)

and the drift time *t* that a charge carrier needs to travel from its origin to the pixel electrodes [15]. The approximation is valid for a constant and homogeneous electric field. In the presence of a magnetic field the diffusion constant can approximately be described with $\mu = \frac{q\tau}{m^*}$ as

$$D'(\omega) = \frac{D(0)}{1+(\omega\tau)^2} = \frac{D(0)}{1+\left(\frac{\mu B}{2\pi}\right)^2} \quad (2)$$

where $\omega\tau = \frac{\mu B}{2\pi}$, with the cyclotron frequency $\omega = \frac{|q| B}{2\pi m^*}$, the mean free time τ between two collisions, $q$and m^* being the charge and the effective mass of a charge carrier in silicon. Given the mobility of $\mu_e = 1350 \text{cm}^2/\text{Vs}$ and $\mu_h = 450 \text{cm}^2/\text{Vs}$ [16] for an electron or a hole, respectively, and $B = 3$ T, which was the largest magnetic field strength that was available to us experimentally, one gets

$$R'(\omega) = 0.9978 \cdot R(0) \quad \text{for electrons} \quad (3)$$

$$R'(\omega) = 0.9998 \cdot R(0) \quad \text{for holes.} \quad (4)$$

These calculations are usually done for the diffusion of gases in gas drift chambers with an external magnetic field. In principle this should also be applicable for semiconductors as well.

3. Experimental setup

The experimental setup is shown in Fig. 3. The detector (green), connected to a Fitpix readout (blue), which was developed at IEAP in Prague [17], was attached to a PVC panel for stability reasons. We were using the version 2.1 of the Pixelman software for data acquisition [18]. The detector part and the radioactive source were drilled into lead blocks (red) and mounted on another PVC panel, also for stability. This was necessary, because the wire connections such as the USB cable for read-out or the LEMO cable for the connection to the power supply, always contain ferromagnetic constituents which tend to move in the magnetic field. This can lead to differences in the distance between the radioactive source and the detector, which would have a big influence on the energy of the α-particle when arriving at the sensor. The number of triggered pixels depends on the energy of an ionizing particle. So, in order to have less variance in the energy of the α-particle for a measurement the stability of the setup is important.

The whole setup was placed inside a common medical MR scanner for magnetic resonance imaging so that the magnetic field lines were parallel to the electric field lines inside the sensor layer. The maximum magnetic flux density was 3000 mT and was measured with a magnetometer with a range up to 2000 mT and an accuracy of ± 20 mT. For the 3000 mT measurement the setup was completely inside the MR scanner. Since at the outermost

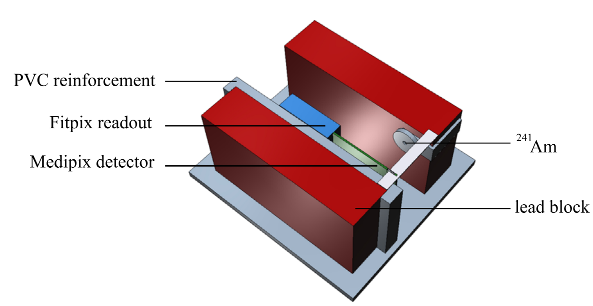

Fig. 3. Experimental setup for the measurements in the magnetic field. Several PVC reinforcements have been attached to avoid movement of the wires or the chip-board due to the magnetic field. This setup has been placed inside the medical MR scanner, such that the magnetic field lines are perpendicular on the sensor layer. (For interpretation of the references to color in this figure, the reader is referred to the web version of this article.)